Ocean Systems Engineering, *Vol. 14, No. 3 (2024) 211-235*
https://doi.org/10.12989/ose.2024.14.3.211

Numerical investigation on hydrodynamic response of a SPAR platform for offshore wind energy

Arya Thomas*[1], V.K. Srineash[1] and Manasa Ranjan Behera[1,2]

[1]*Department of Civil Engineering, Indian Institute of Technology Bombay, Powai, Maharashtra, 400076, India*
[2]*Centre for Climate Studies, Indian Institute of Technology Bombay, Powai, Maharashtra, 400076, India*

(Received July 2, 2024, Revised August 22, 2024, Accepted September 10, 2024)

Abstract. Th COP28 has emphasized the governments to speed up the transition away from fossil fuels to renewables such as wind and solar power in their next round of climate commitments. The steady and less turbulent wind over the ocean draws increased attention of governments, industries and researchers on exploring advanced technologies to extract energy from offshore wind. The present study numerically investigates the hydrodynamic behavior of a SPAR-type Floating Offshore Wind Turbine (FOWT) under various wave conditions and mooring line configurations. One of the major focuses of this study is investigating a freak wave's impact on a FOWT and determining its extreme responses. The study investigates the structural response under various wave impact for different configurations of mooring lines. The present study examines the wave-structure interaction under regular and freak wave conditions using numerical modelling approach. During the study, it is ensured that the natural frequency and wave induced motions of SPAR are inline with the experimental studies; thereby increasing the confidence in using the numerical model and domain for this investigation. The study considers the behaviour of slack and taut mooring arrangements under these wave conditions. The study observed that a taut mooring configuration can be efficient in restraining the FOWT motions, especially under a freak wave scenario. The Froude-Krylov force shows a non-linearity due to the non-uniform profile of the platform under all wave conditions. Overall, the study contributes to determining the performance of the mooring configurations under different wave conditions.

Keywords: floating offshore wind turbine; freak wave; mooring lines; slack moorings; SPAR; taut-moorings

1. Introduction

The emission of green-house gases to the environment from burning fossil fuels is creating an urgent need to prioritize our energy usage. These green-house gases have adverse effects, leading to severe pollution, health hazards and changes in the global climate. “Transition to clean and renewable energies is an essential solution to achieve the Sustainable Development Goals (regarding affordable and clean energy) toward 2030” - addressed by the United Nations. In the recent COP28, the deal committed all the signatory countries to move from carbon energy sources ‘in a just, orderly and equitable manner’, to mitigate the worst effects of climate change, and reach net zero by 2050 (Morton *et al*. 2023).

*Corresponding author, Ph.D. Student, E-mail: aryathomas0008@gmail.com

http://www.techno-press.org/?journal=ose&subpage=7 ISSN: 2093-6702 (Print), 2093-677X (Online)

A decade since, the developments in the energy sector have shifted to renewable energies, especially from the vast oceans. Due to its less turbulent, steady and higher velocity (Esteban *et al*. 2011), offshore wind is gaining a lot of attention in the field of renewable energy. In order to place the offshore wind turbine, there is a need for a sub-structure/ foundation/ platform. Based on the water depth available on the offshore region, the foundations can be classified into two types: - fixed foundations and floating platforms with mooring systems. Fixed foundations are the ideal choice due to its lesser cost for a water depth between 20 to 50 m (Atcheson *et al*. 2016). However, for sites that are further away from the coast where the wind energy is greater than the near shore, floating platforms with moorings would be a suitable option. Such platforms can be used in locations where the water depths can be up to hundreds of meters. The concept of offshore wind turbine platforms is adopted from the conventional oil and gas industries. In fixed platforms, jackets and monopiles are widely used with advanced technologies to understand their dynamics. The developments in the design of floating offshore platforms still need greater understanding, as their dynamics are complex due to the coupled effects of aero-hydro-servo-mooring combination. Floating platforms like Semi-Submersible Platforms (SSP), tension leg platforms (TLP), and SPAR are adopted for placing offshore wind turbines. Recently, new platform concepts like T-Omega, SATH and TetraSPAR have been looked upon in the field of floating offshore wind (Edwards *et al*. 2023).

One of the primary concerns for any FOWT design is its stability. The SPAR platform is a ballast-stabilised sub-structure. It is a long-deep drafted cylindrical structure where stability is achieved by using ballast thus lowering the center of gravity (COG) far below the center of buoyancy (COB). This helps in attaining stability (Proskovics 2015). The SPAR platform has a simple design and is economically cost-effective, thus they are considered as a better option for deeper waters.

Mooring lines play a crucial role in FOWT design ensuring its survivability and stability, as they are used to station keep these platforms, thus avoiding drifting and enhancing stability during operational conditions. They are anchored to the seabed from the fairleads of the platform. These lines differ in materials and configurations/ arrangements. Fundamentally, there are four different types of mooring line configurations: catenary, taut, semi-taut and tether, which are mainly comprised of chain links and wires from steel. Out of these, the slack and taut mooring arrangement are widely considered for FOWT for various practical reasons (Barrera *et al*. 2019). In case of slack mooring arrangement, the line takes up the profile of a catenary section and thus, does not allow the vertical loads. Hence, requiring sufficiently long line length thereby increasing the footprint (Barrera *et al*. 2019). These factors have made the researchers look for alternate mooring line configurations like taut mooring lines, especially for FOWTs. Furthermore, factors such as reduction of mooring line loads and fatigue damage during the power productions motivate researchers and engineers to understand the behaviour of FOWT for taut mooring configurations. The design of the mooring line is a critical parameter for any floating offshore platform. The need for studies focusing on mooring line configuration for FOWT has been emphasized in the earlier works (Kota *et al*. 1999, Agarwal and Jain 2003, Tang *et al*. 2007, Song *et al*. 2012, Borlet 2016, Azcona and Vittori 2019, Ghigo *et al.* 2022). The research outcomes based on the study conducted by Xiang *et al*. (2022) indicate that a thorough understanding of the dynamics of the taut mooring line is essential as it can potentially replace the catenary lines, thus reducing the overall levelized cost of energy (LCOE). As a preliminary investigation, Arya *et al.* (2023a) conducted an experiment on a simple SPAR structure restrained using soft horizontal mooring lines. These results are then employed to conduct validation studies for a numerical tool, which showed good agreement. The authors concluded that for the preliminary analysis of floating offshore platforms, soft horizontal mooring lines can be adopted to station keep the platform from drifting without affecting the responses.

Though the history of wave-structure interaction studies is sufficiently mature. Nevertheless, understanding the behaviour of FOWT especially with freak wave is considered important considering the prevailing implications due to climate change and to examine the robustness of the system. A freak wave is a wave or wave train with a wave height greater than twice the significant wave height (Haver and Andersen 2000, Sand *et al*. 1990, Brunn 1994). The freak wave considered in the present study is the famous Draupner wave that happened on 1st January 1995. This is the only freak wave that has been recorded by an offshore platform. The wave parameters for the observed Draupner freak wave are H_{max} = 25.6 m and time period (T_w) of 12s (Haver and Andersen 2000).

Like any other moored platforms, FOWTs may also experience potential damage when subjected to freak waves (Li *et al*. 2023, Li *et al*. 2024). Freak waves on FOWTs can significantly affect their power production (Li *et al*. 2020). Similarly, Arya *et al*. (2023b) performed a numerical investigation on a SPAR FOWT subjected to freak wave time series for a non-operational wind turbine case with slack mooring arrangement. A few notable observations based on this study are the impact of freak wave has amplified the pitch motion of the FOWT and there is a significant reduction in the air-gap that may induce additional aerodynamic loads in the operational case.

Physical model experiments are inevitable to understand and comprehend the wave-structure interaction process and the hydrodynamic responses. However, there are limitations with respect to the test facilities to achieve proper similitude. In general, there are restrictions in the hydrodynamic test facilities such as unavailability of required water depth/tank width. Therefore, researchers try to overcome these limitations with modified mooring arrangement (Xu and Day 2021, Yang *et al*. 2022) or by choosing a lower scale ratio (Luo *et al*. 2020, Ruzzo *et al*. 2021).

In the present study, the responses of a SPAR-type FOWT are investigated for regular and freak wave conditions. The OC3-Hywind SPAR housing the NREL 5 MW wind turbine is taken as the study platform. The model is proposed by Jonkman (Jonkman 2010). The mooring configurations considered in the present study are taut and slack moorings. Validation cases are conducted to determine the accuracy of the chosen numerical tool. Then a few wave-structure interaction studies are performed for the selected wave conditions to investigate the responses and forces acting on the platform. The main objective of this study is to explore the efficiency and performance of the SPAR FOWT for different mooring line configurations under wave impacts in restricted hydrodynamic test facilities.

2. Numerical Investigation

2.1 Numerical model

The study investigates the hydrodynamic response of a SPAR-type FOWT under regular wave and freak wave for different mooring arrangement. The numerical investigation is carried out using ANSYS AQWA that adopts the panel (boundary) method to solve the equation of motion (Chakrabarti 1987) given in Eq. (1).

$$[M + A]\{\ddot{x}\} + [C]\{\dot{x}\} + [K]\{x\} = \{F\} \tag{1}$$

where, M represents the mass matrix, A is the added mass matrix, C indicating the damping matrix, K is the restoring stiffness matrix, x represents the displacement vector, $\dot{x}$ is the velocity vector, $\ddot{x}$

is the acceleration vector, F is the external hydrodynamic force vector.

The boundary value problem can be solved using the following set of boundary conditions: kinematic and dynamic free surface boundary conditions, body boundary condition and bottom boundary condition given in equations 3-6 respectively along with the Laplace equation (equation 2) as the governing equation (Chakrabarti 1987)

$$\nabla^2\varphi = 0 \tag{2}$$

$$\frac{\partial\eta}{\partial t} = \frac{\partial\varphi}{\partial z} \; @z = 0 \tag{3}$$

$$\frac{\partial\varphi}{\partial t} + g\eta = 0 \; @z = 0 \tag{4}$$

$$\frac{\partial\varphi}{\partial n} = V.n \tag{5}$$

$$\frac{\partial\varphi}{\partial n} = 0 \; @z = -d \tag{6}$$

where, z is the vertical distance from SWL to seabed, η is the wave elevation, n is the unit normal, V is the body velocity, φ is the velocity potential and d is the water depth.

2.2 Methodology

The study is aimed at conducting a comprehensive parametric numerical investigation to understand the hydrodynamic responses of the SPAR platform housing wind turbine. The study also investigates the wave impact on FOWT with different mooring line configurations. Experimental results from Xu and Day (2021) have been considered for performing the validation exercise. The study adopted a scale ratio of 1:74 to accommodate the model in the experimental facility (wave flume) with a maximum water depth (d) of 2 m. Thus, the authors could achieve the required draft in model scale, but the mooring configuration had to be changed due to the restrictions in the wave flume. The authors have adopted an asymmetric mooring configuration with the angle between the adjacent mooring lines as 60^0, 150^0, 150^0. A similar mooring arrangement is considered for the present study. For the taut mooring configuration, the vertical angle adopted is 45^0. The line length and angle with seabed are changed by keeping other material properties same as slack line. For further insights on the experimental investigation, readers are advised to check Xu and Day (2021). The details about the SPAR model and mooring arrangement considered in the present study are stated in Table 1. The numerical domain adopted for the present study is 19 m long, 4.6 m wide and with a water depth of 2 m.

A frequency domain investigation is used for the hydrodynamic analysis of the SPAR-type FOWT. A linear potential flow approach is adopted using the panel method to solve the equation of motions (Nallayarasu and Kumar 2017, Aggarwal *et al.* 2017). The SPAR FOWT is modeled in ANSYS AQWA as a surface body along with the mooring lines modeled as a non-linear catenary system for the slack configuration considering the length, axial stiffness, weight of the mooring line and solved using catenary equations. A linear stiffness system for the taut mooring configuration is used by describing the stiffness and unstretched length. The structure to which the cable is attached will experience a force of varying magnitude and direction, which is proportional to its extension (AQWA 2018). The mooring arrangements are shown in Fig. 1.

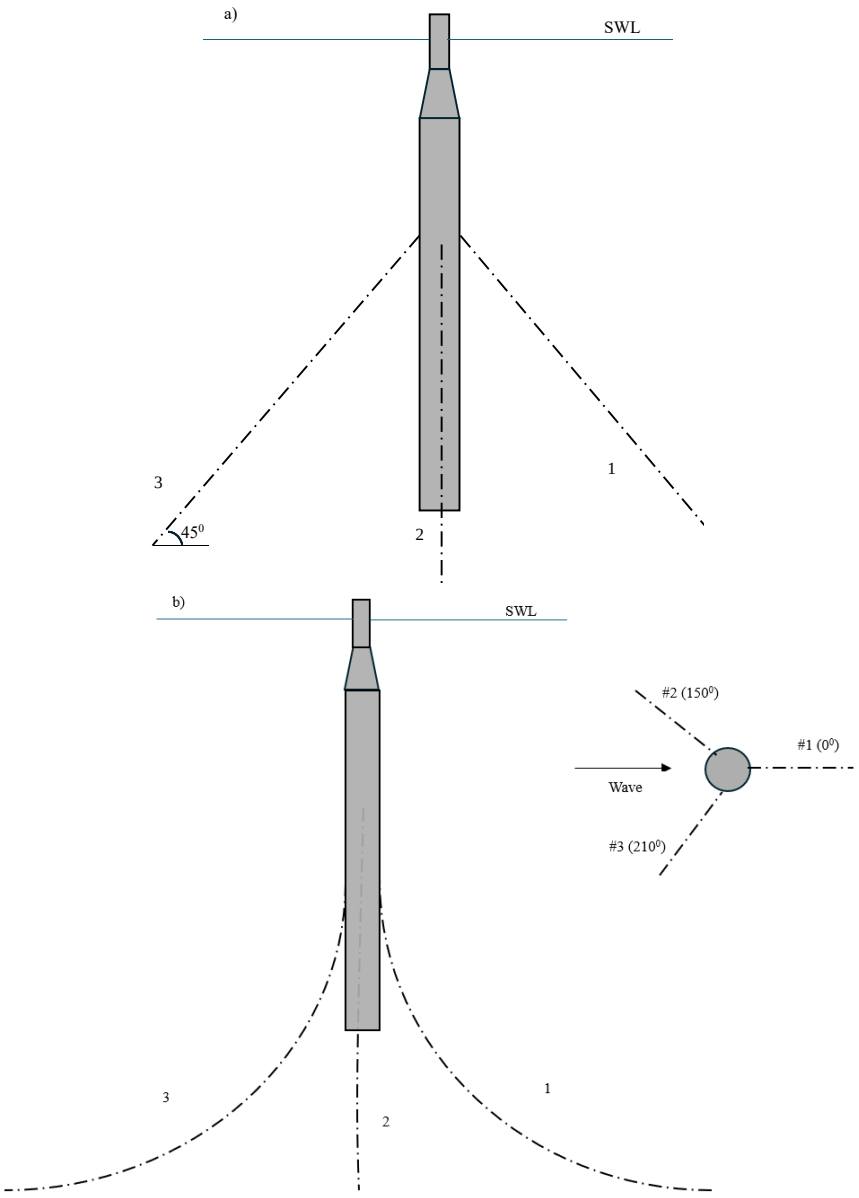

Fig. 1 FOWT model adopted for present study with (a) taut mooring and (b) slack mooring configuration

The numerical investigation to determine the hydrodynamic responses using ANSYS AQWA is performed for d/λ = [0.07,0.08,0.09,0.11,0.128,0.15,0.184,0.227,0.288,0.37,0.52,0.74,1.15,2.05 ,3] and H/λ = 0.0012-0.03. The present study adopts two types of regular waves: linear and Stoke's second order, based on periodic water wave theory as the function of H/gT^2 and d/gT^2 (Le Méhauté 1976). The test matrix for regular waves consists of 16 wave combinations from the above d/λ and H/λ ranges. The study also incorporates the investigation of the response of FOWT under freak

Table 1 Model and mooring properties adopted in the present study

Model properties	Values
Total draft of the platform, L (m)	1.5
Diameter above tapered section, D (m)	0.08
Diameter below tapered section (m)	0.1175
Distance to top of tapered section from SWL (m)	0.05
Distance to bottom of tapered section from SWL (m)	0.15
Mass of platform including ballast (kg)	14.65
CG from keel (m)	0.4
Roll/Pitch inertia about CG (kgm^2)	6.11
Number of mooring lines	3
Water depth, d (m)	1.8
Angle between adjacent lines (^{0})	0/150/210
Unstretched mooring line length (m)	3.3
Diameter of mooring line (m)	0.00125
Equivalent mooring line weight (kg/m)	0.011
Equivalent mooring line extensional stiffness (N/m)	1.4E5
Distance to fairleads from SWL (m)	0.87
Anchor depth (m)	1.8

Table 2 Non-dimensional parameters considered in the study

Parameters	Range
d/λ	0.07-3
D/λ	0.004-0.11
H/λ	0.0012-0.03
H/D	0.125-0.5

wave (Draupner wave in this study). The freak wave time series is fed as an external input into the tool. As the potential flow theory neglects the viscosity, the viscous damping coefficient from the free decay test of Xu and Day (2021) is taken as an external input for precisely obtaining the response of SPAR-type FOWT with the mooring configurations in the validation study (Nallayarasu and Kumar 2017). Table 2 details the non-dimensional parameters considered in the study.

The hydrodynamic responses viz., surge, heave and pitch motions of the platform and the associated forces viz., Froude-Krylov force are evaluated. Estimation of these responses will provide adequate information on the design of FOWT and help the designers further.

The present parametric investigation uses a numerical approach that will set as a precedence to perform the physical model test campaigns that are planned in the wave flume of the Department of Civil Engineering, Indian Institute of Technology Bombay, India. Therefore, for the present study, the model setup in the numerical domain has been devised accordingly for a scale ratio of 1:80. This numerical study is aimed to derive better understanding on the hydrodynamic responses of the FOWT when subjected to regular waves. Also, to check the robustness of the designed system under very extreme event, a freak wave scenario is examined. Therefore, a detailed parametric study has been carried out to understand the responses of the FOWT.

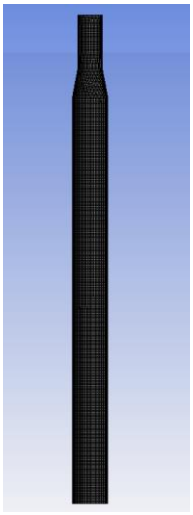

Fig. 2 Meshed SPAR model considered in the present study

2.3 Mesh convergence study

In order to determine the required mesh size suitable for numerical investigation, a mesh convergence study is performed. An unstructured non-uniform mesh generation scheme is adopted in the numerical tool to attain the required discretised model. The model's outer surface is divided into panels with the adopted element size. The mesh convergence studies are conducted for three different mesh sizes of 0.02 m, 0.01 m, and 0.005 m. An illustration of the meshed model with the hydrodynamic panels is shown in Fig. 2. The details of the mesh convergence study for the heave RAO are illustrated in Fig. 3. Contrasting to the higher mesh sizes (i.e., 0.02 m), the difference in the peak value of heave RAO for fine meshes (i.e., 0.01 m and 0.005 m) show very slight variation (~0.07%) and they exhibit close match. The comparative study between these numerical results and the experimental study by Xu and Day (2021) depicts reasonable correlation for heave RAO. In addition to this, the mesh convergence study considering heave damping coefficients (Fig. 4) is examined as linear damping and external stiffness also influence the RAOs (Riggs 1992, Ramachandran *et al.* 2013). Since AQWA solver sets the frequency range in accordance with the mesh size, finer the mesh, the interval of frequency range also becomes finer, and more additional frequencies are included by the solver (AQWA 2018). The same aspect is reflected in Fig. 4.

Thus, based on this mesh convergence study, the mesh size of 0.005 m is adopted for further parametric studies. It is clarified here that the wave parameters considered in the present study are as mentioned in Table 2.

2.4 Validation study

The numerically simulated heave and pitch RAOs are compared with the experimental results of Xu and Day (2021) as shown in Figs. 5(a) and 5(b) respectively. The study observed a close match for heave and pitch RAOs with the experimental results. Further, a regular wave impact on the SPAR is also compared for the heave time series for $f/f_{nz} = 2.65$, H/D=0.425. The numerically simulated

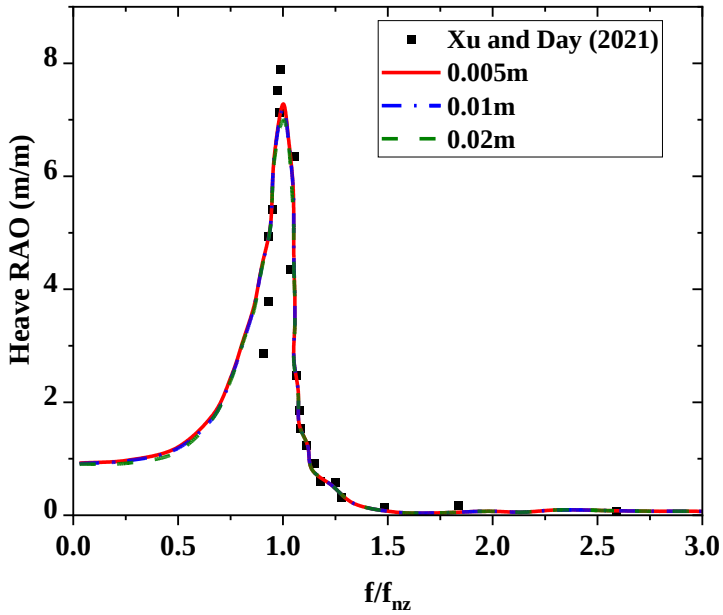

Fig. 3 Comparison of numerical heave against Xu and Day (2021) for mesh convergence study

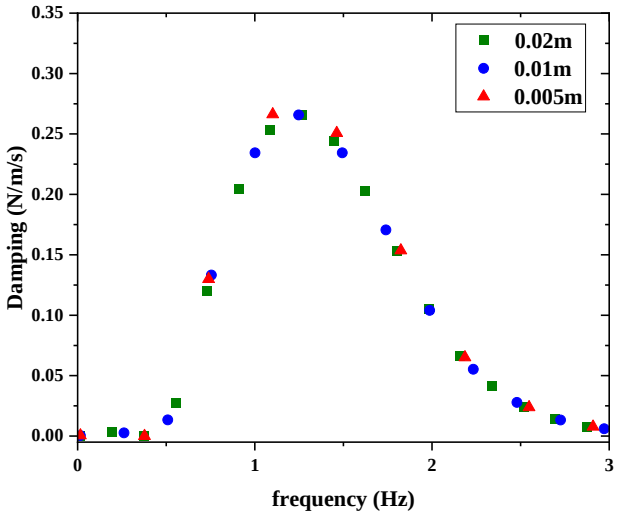

Fig. 4 Comparison of numerical heave damping for mesh convergence study

heave response showcases a good agreement with the physical model test results (Fig. 6) for the case where the wave interacts with the SPAR platform. Further, the peak heave RAO obtained from Xu

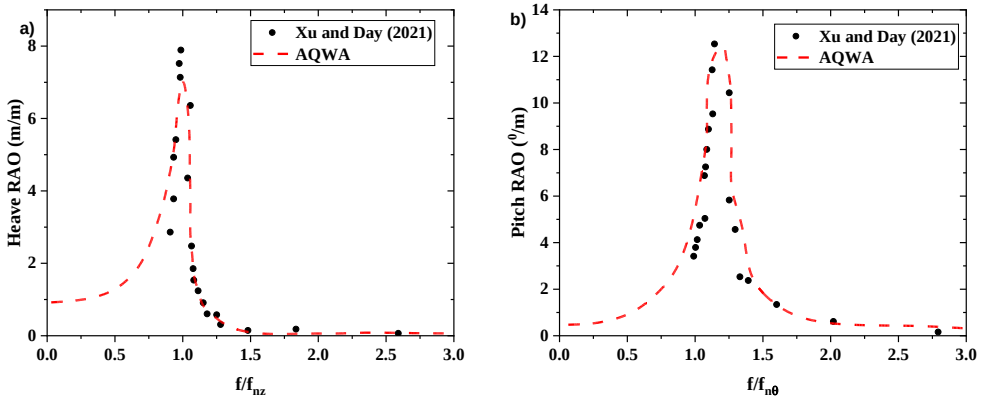

Fig. 5 Validation study on (a) Heave and (b) Pitch RAOs

and Day's (2021) experiment is 8 m/m. However, the present numerical results are noticed to have lower peak in heave response (6.9 m/m). Such deviation in the values between numerical and experimental values are also seen in earlier studies. It can be argued that the effect of side walls and other non-linear interactions in the case of experiments could be a reason to perceive higher responses during physical model studies (Nallayarasu and Kumar 2017, Hegde and Nallayarasu 2023). The performed validation study further increases the confidence of adopting the numerical tool to study the wave structure interaction process for the FOWT.

2.5 Free decay tests

A numerical free decay test is conducted to determine the natural period in heave and pitch direction. For this, an initial oscillation (displacement or rotation) in the respective directions is given to the model. The damping ratio, restoring stiffness values, natural frequency are derived from the free decay tests using the linear damping Eqs. in (7)-(10).

$$\delta = \frac{1}{n} ln \frac{z_0}{z_n} \tag{7}$$

$$\zeta = \frac{1}{\sqrt{1+\left(\frac{2\pi}{\delta}\right)^2}} \tag{8}$$

where, δ indicates the logarithmic decrement, z_0 indicates the initial peak amplitude, z_n indicates the peak amplitude at n^{th} cycle, ζ is the damping ratio, C is the damping coefficient, K_{zz} and $K_{\theta\theta}$ are heave and pitch restoring stiffness respectively, ρ indicates the density of water, g indicates the acceleration due to gravity, A_w indicates the water-plane area, ∇ indicates the volume displaced and GM is the metacentric height.

From the linear damping equations, the natural frequencies of the platform can be determined from

$$\omega_d = \frac{2\pi}{T_d} \tag{9}$$

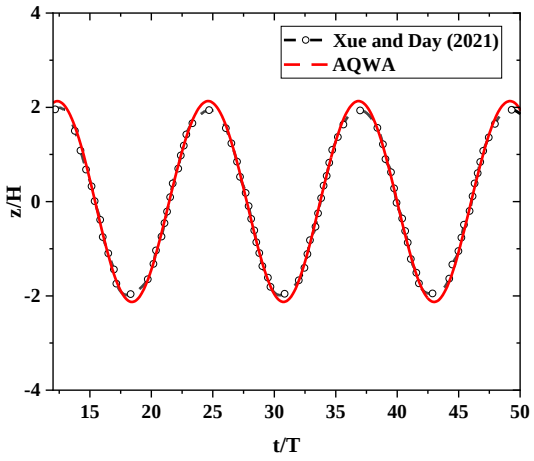

Fig. 6 Validation study on heave time series

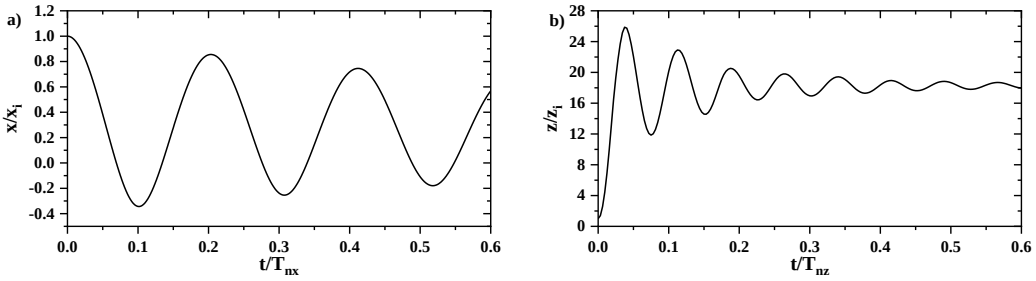

Fig. 7 Moored free decay time series for (a) Surge and (b) Heave

Table 3 Comparison of natural frequency in heave and for SPAR only

DOFs	AQWA	NREL Full scale
	f_n (Hz)	
Heave	0.033	0.032
Pitch	0.035	0.034

$$\omega_n = \frac{\omega_d}{\sqrt{1-\zeta^2}} \tag{10}$$

where, ω_n is the natural frequency, ω_d indicates the damped natural frequency and T_d indicates the damped time period.

The time series of slack moored free decay for surge and heave DOFs is plotted in Fig. 7. The drag coefficient of the platform and mooring lines 0.6 and 0.025 respectively (Xu and Day 2021)

Table 4 Linear Damping ratios

DOFs	AQWA	Xu and Day (2021)
Surge	0.021	0.017
Heave	0.02	0.028
Pitch	0.022	0.023

are considered in the decay tests. Table 3 shows the comparison of natural frequencies in heave and pitch DOFs for the unmoored SPAR. The natural frequencies obtained for NREL full scale are taken from Ramachandran *et al.* (2013). The linear damping ratios for surge, heave and pitch are also compared in Table 4. The static offset tests in each DOFs are not performed as the mooring line properties are not varied from Xu and Day (2021) model and present study focus mainly the hydrodynamic response of SPAR FOWT.

2.6 Response amplitude operators

In the coming sections, the regular wave investigations are conducted to determine the dynamic characteristics of the FOWT for both the mooring line configurations (taut and slack). A regular wave analysis is important for any offshore platform, as it provides a clear understanding on the variation of the responses subjected to monochromatic waves (Nallayarasu and Kumar 2017). In the present study, the dynamic response of the platform is evaluated in terms of Response Amplitude Operators (RAOs) (Eq. (11)) (Chakrabarti 1987) in the frequency domain.

$$RAO_i = \frac{\zeta_i(\omega)}{a} \tag{11}$$

where, ζ_i is the i^{th} DOF depending on the angular frequency ω and a denotes the wave amplitude.

RAOs are typically the frequency response function which helps to determine the responses of the platform for unit wave amplitude (Chakrabarti 1987, Nallayarasu and Kumar 2017). Fig. 8 gives the RAOs of SPAR for surge, heave and pitch per unit wave amplitude for the moored SPAR FOWT. The influence of mooring line properties is also included in the RAOs calculation (Rajeswari and Nallayarasu 2022). It is noticed that the SPAR has slightly higher responses in surge and pitch. It is observed that the peak of the responses occurred when the wave period is closer to the natural periods of the platform in surge and heave; there is a slight shift in pitch (Fig. 8), which is also seen in mesh convergence study.

3. Results and discussions

3.1 Effect of variation in regular wave parameters for taut mooring arrangement

The wave-structure interaction of regular wave parameters with the FOWT is investigated in this section. In Fig. 9, the maximum amplitudes of the motions have been normalised with corresponding incident wave heights (H) and wave periods (T) over natural period (T_{ni}) of FOWT in the respective directions. The results demonstrate that the surge and heave responses have increased with the increase in wave height. It is also evident from Figs. 9(a) and 9(b) that the taut mooring configuration is restraining the surge of the platform significantly. For the lower values of the wave period (T/T_{nx} = ~0.025-0.1; T/T_{nz} = ~0.3-0.6), the increment in surge and heave are not appreciable. There is a

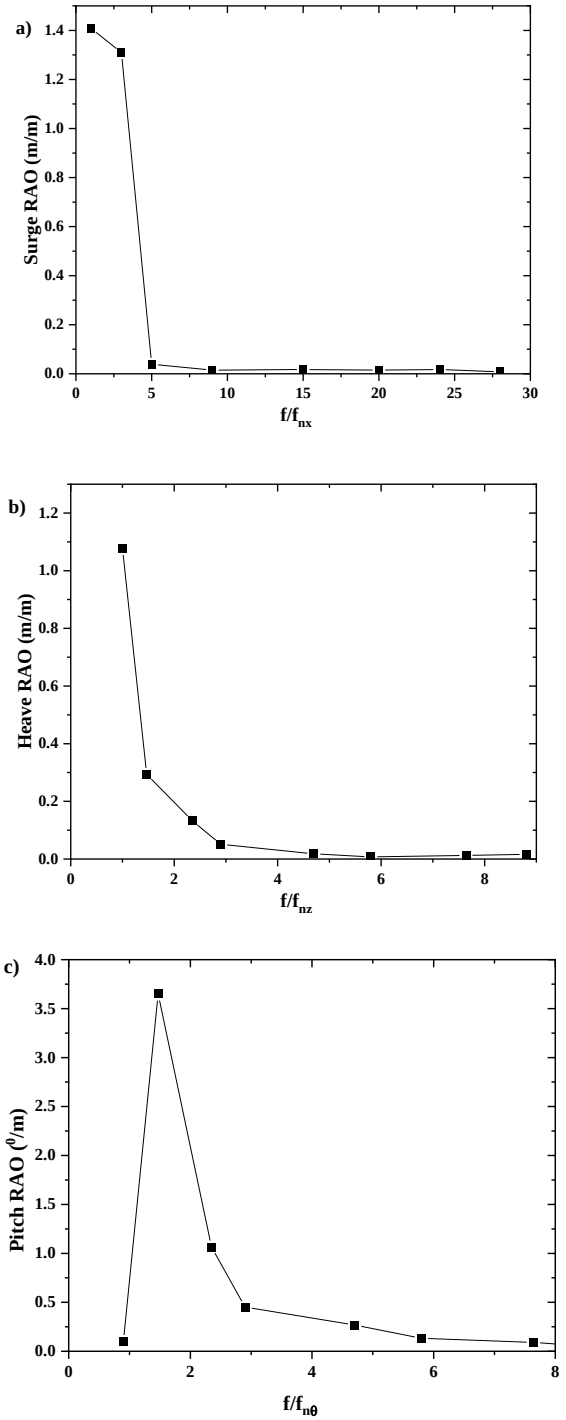

Fig. 8 Response Amplitude Operators from the present study (a) Surge, (b) Heave and (c) Pitch

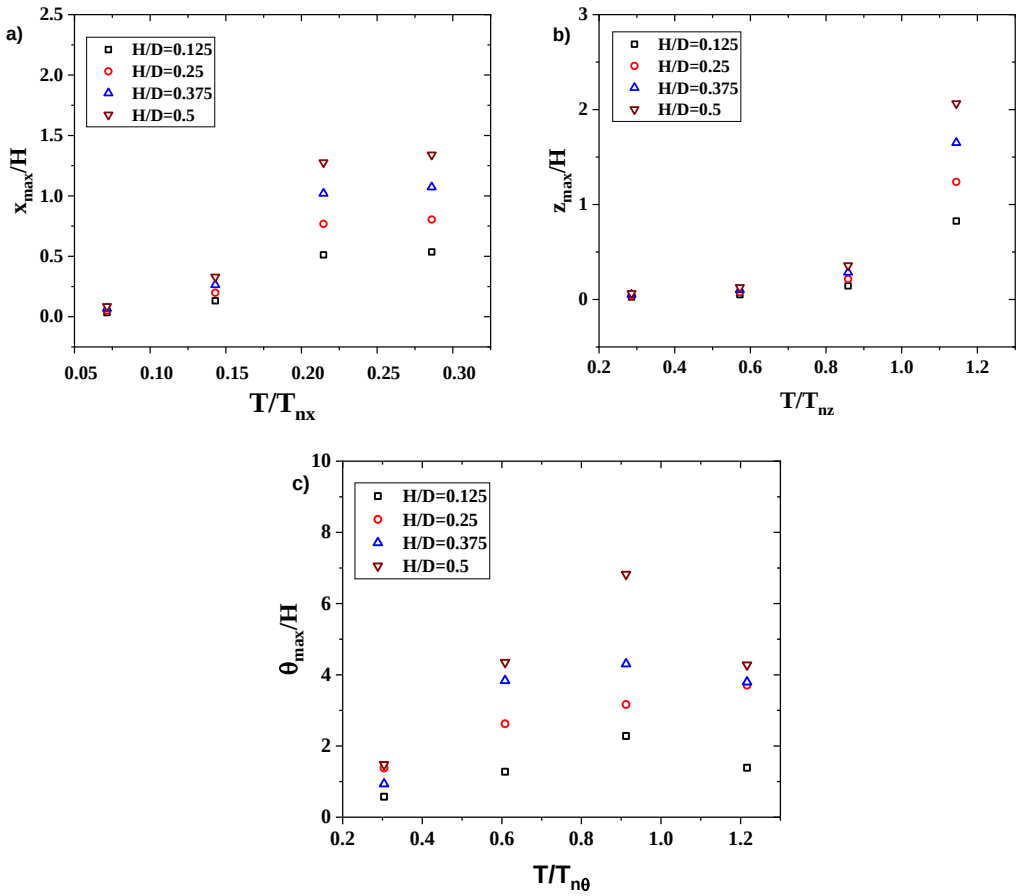

Fig. 9 Variation of normalized maximum amplitude of responses for a taut mooring arrangement with $k=k_p$ (a) Surge, (b) Heave (c) Pitch (where, T_{nx} is the surge natural period, T_{nz} is the heave natural period, $T_{n\theta}$ is the pitch natural period)

gradual increase in the heave response as the wave periods approach closer to the heave natural frequency. This increase is prominent at T/T_{nz} = 1.18 (Fig. 9(b)). The resonant case of T/T_{nz} = 1 is not presented as the wave parameters considered are slightly away from heave natural frequency. Nevertheless, this shall be considered for future investigations. The pitch motion response of the SPAR platform is presented in Fig. 9(c). The results indicate that the pitch response has an increasing trend closer to its natural frequency. This can be perceived by interpreting Fig. 9(c), where the maximum response is observed at $T/T_{n\theta}$ = 0.9 (Fig. 9(c)). It is also observed that the pitch value exceeds its critical value (10-15^0) (Collu and Borg 2016) for certain wave combinations making the wind turbine's operational condition difficult. This scenario further points to the scope of applicability of additional dampers in the pitch DOF for a taut mooring configuration.

3.2 Effect of variation in regular wave parameters for slack mooring arrangement

Fig. 10 compares the variation in the responses under different wave parameters for a slack

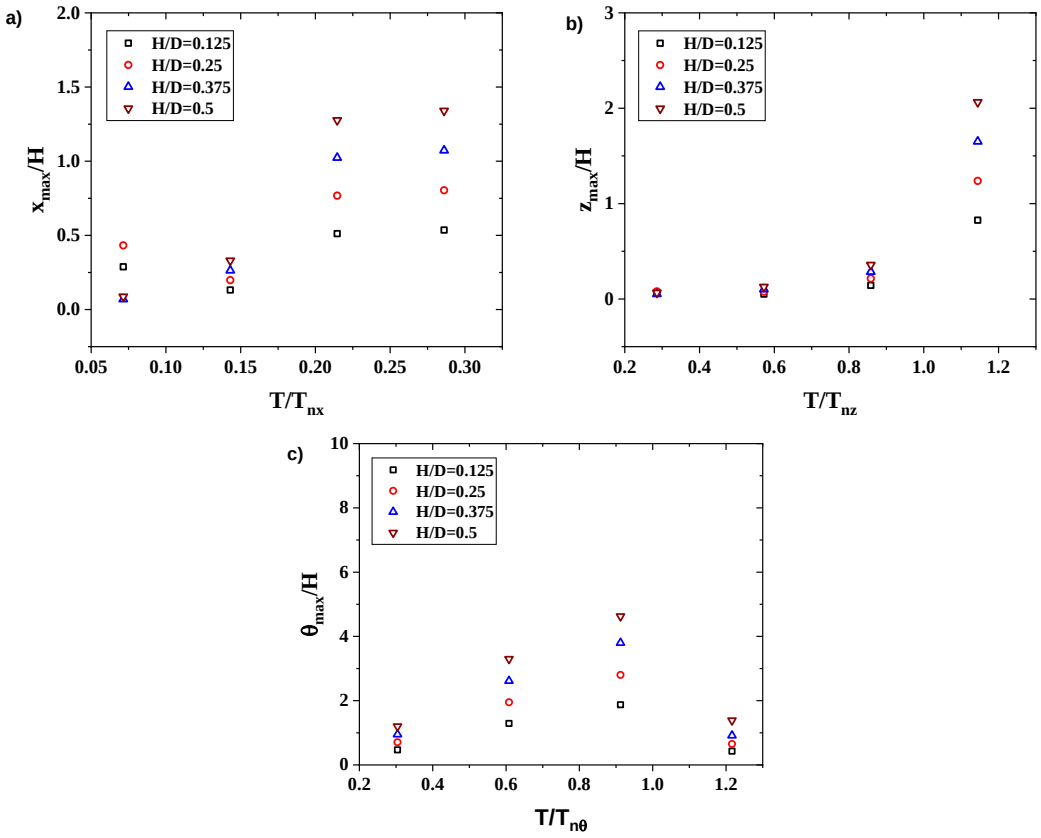

Fig. 10 Variation of normalized maximum amplitude of responses for a slack mooring arrangement (a) Surge, (b) Heave (c) Pitch

mooring line configuration. The mooring line parameters are adopted from the OC3 Hywind project (Table 1). Fig. 10(a) and 10(b) shows a stable increment as the wave parameters increases in the surge and heave directions. In surge, there is an increase in amplitude when the wave height is less. The pitch motion shows a decreasing trend beyond $T/T_{n\theta}$ = 0.9. But the motions get significantly amplified when the wave period is closer to the pitch natural period of FOWT.

Comparing Figs. 9 and 10, it is understood that the surge motion in slack mooring configuration is significant for the low-frequency range (T/T_{nx} = ~0.025-0.15). This can be due to the amplification of surge (mainly the drift) by the interaction of lower-period waves (Li *et al.* 2020). This trend is not observed in a taut mooring configuration, indicating that by adopting a taut arrangement, the slow-drift motion of the platform can be minimized. In contrast, the pitch shows a reduced magnitude for slack moored configuration for all the wave periods considered in the study. The results indicate a 2% reduction in pitch response for $T/T_{n\theta}$ = 0.6 and about ~5% reduction for $T/T_{n\theta}$ = 0.9 in pitch for slack configuration compared to taut moored configuration. Similar variation in responses under different wave parameters are reported in past literature (Nallayarasu and Saravanapriya 2013, Brito *et al.* 2020, Rony *et al*. 2023). It can be reasoned that the additional un-stretched length of the slack mooring line contributes to dampening the pitch motion in addition to the self-weight of the mooring line in case of slack condition.

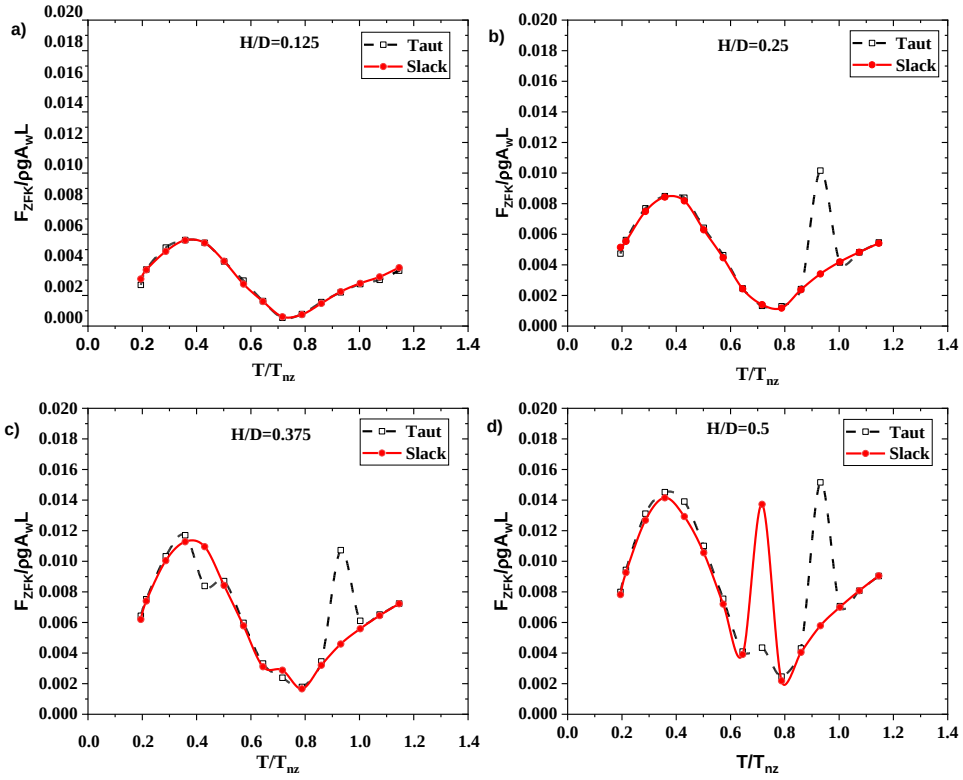

Fig. 11 Variation of maximum Froude-Krylov force in heave direction with varying wave parameters (a) H/D = 0.125, (b) H/D = 0.25, (c) H/D = 0.375, (d) H/D = 0.5 (where, A_W is the water plane area, L is the draft of the platform)

3.3 Effect of variation in regular wave parameters on Froude-Krylov force for different mooring configurations

The total wave excitation force on an offshore platform is the sum of the Froude-Krylov force and diffraction forces. It is always essential to determine these loads to design an offshore platform. The variation of these forces in heave direction with regular wave parameters and different mooring line configurations have been presented in Fig. 11. The maximum force amplitude has been non-dimensionalized in accordance with Kim *et al.* (2021). From Fig. 11(a), it is evident that the wave parameters have a substantial effect on the heave Froude-Krylov force for the OC3 Hywind SPAR. The adopted SPAR for the present study falls under the Froude-Krylov region for the considered wave periods (Chakrabarti 1987). The dominating effect of the Froude-Krylov force is because of the diameter to wavelength ratio, ($D/\lambda < 0.2$) which falls in Froude-Krylov force regime for the wave parameters considered in the present study. The study also observed that there is an increment of Froude Krylov force with an increase in wave height.

From Figs. 11(b)-11(d), it is evident that a peak in hydrodynamic force is observed for higher wave heights, and this is pronounced in frequencies closer to the natural frequency ($T/T_{nz} = 0.93$) of

the FOWT for taut mooring arrangement. The examination on the Froude-Krylov force time history depicts a non-linear profile at the aforementioned regions (Ghafari *et al*. 2019, Jang and Kim,2020). Unlike the conventional SPARs, the OC3 Hywind SPAR platform has a non-constant water plane area (a tapering section is provided to reduce the wave loads) along its hull and the irregularity in the shape of hull can cause variation in the motion. As a result, Froude Krylov force is seen to be significantly reduced at T/T_{ni} = 0.65 – 0.8. Similar trend is perceived by Hegde and Nallayarasu (2023). The presence of non-linear or higher order terms in Froude Krylov force, 2nd order diffraction loads and Morison drag force due to the instantaneous wetted surface of the platform can also contribute to such non-linear behaviour (Kim *et al.* 2018, Jang and Kim 2020, Kim *et al.* 2021). However, the present study considers linear potential theory and hence does not account for the non-linear loads beyond the still water level.

It can be concluded that the variation of heave Froude-Krylov force for different mooring arrangements is similar and insignificant (~0.05 – 0.5%) due the less influence of mooring arrangement on the SPAR motion responses, except at T/T_{nz} = 0.93, up to H/D = 0.25 for taut mooring. However, an anomaly is observed for the slack mooring arrangement for H/D = 0.5 at T/T_{nz} = 0.7 (Fig. 11(d)). This behaviour could be due to the change of the slack condition of the line for higher wave heights, causing a modification in the motion response of the SPAR in heave direction leading to the varied Froude-Krylov force. An investigation on the influence of lower period (T/T_{nz} < 0.19) is recommended to test the SPAR's behaviour in the transition zone, thus determining the influence of Froude-Krylov force regime on OC3 Hywind SPAR and mooring arrangement on the motions.

3.4 Effect of freak wave impact on different mooring configurations

Apart from the investigation based on regular and extreme wave interaction on floating platforms, freak wave impacts on floating platforms are observed to be necessary. The freak waves occur anywhere (inshore or offshore) and at any time (calm sea or storm sea states). Owing to their exceptionally destructive and unpredictable nature, these have resulted to many ocean/ marine accidents world-wide (Zeng *et al.* 2023). The freak wave used in the present study is the Draupner wave. During the extreme events, the turbine is shut from producing power, but the platform interacts with the waves. Thus, a proper hydrodynamic investigation is required for the design of FOWT under freak waves. The freak wave-structure interaction is carried out to examine its impact on the two mooring arrangements adopted. Fig. 12 illustrates the normalised Draupner wave profile that is fed as a user-defined input file into the tool.

Fig. 12 depicts the normalized time series of FOWT motions under the Draupner wave. It points to the fact that the effect of the Draupner wave primarily happened at its peak and sustained for t/T_w ~2. From Fig. 13(a), it is seen that the surge response in slack mooring configuration is significantly higher compared to the taut mooring arrangement. This can be mainly due to the strong drifting of the FOWT in the direction of freak wave due to the unstretched length of the slack mooring lines. Also, the surge and freak wave are in-phase for the slack configuration, i.e., the maximum surge amplitude (~1.3 m/m) is seen when the maximum crest of the Draupner wave has occurred (t/T_w = 21). This pattern is not visualized in the case of the taut arrangement. Further, it is observed that there is also a strong interaction of the wave after the peak is passed by on the platform. From the heave response (Fig. 13(b)), both the mooring arrangements show comparable results with trivial differences (0.02%) in amplitude. The marginal difference may be due to the forces in the vertical

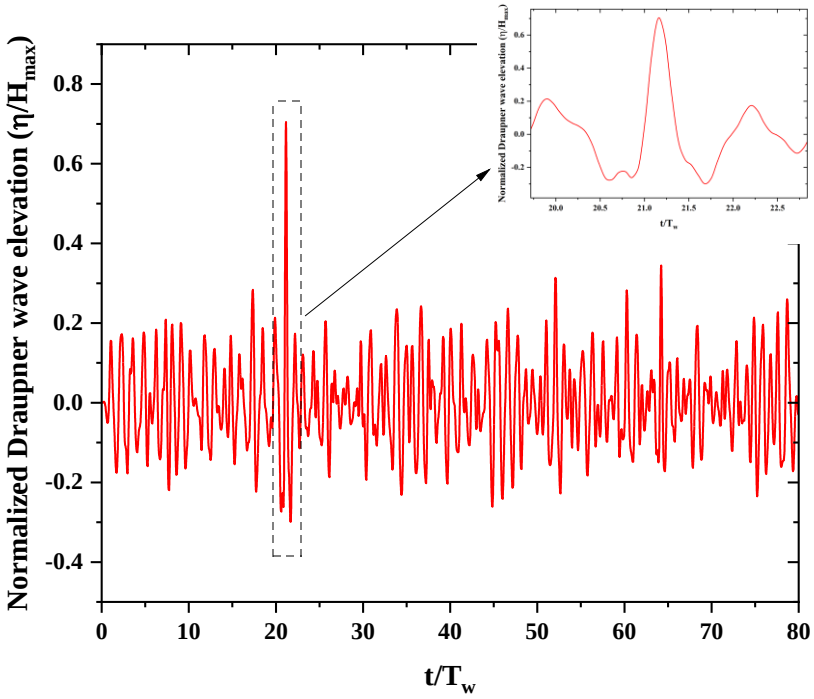

Fig. 12 Observed wave elevation time series of Draupner wave (normalised by max. wave height and period)

plane getting resolved efficiently by the moorings, leading to less motion. But there is an out-phase trend in heave and Draupner wave peak amplitudes. This indicates that the peak heave response occurred during the trough of the Draupner wave. One of the possible causes for this phenomenon can be due to the nonlinear coupling effect between the heave and pitch (Qu *et al.* 2020).

The pitch responses (Fig. 13(c)) show a behaviour like the surge in the slack mooring configuration. It is evident that there is a significant pitch after the Draupner wave interacts with the FOWT, in turn leading to the instability of the platform. This may be also due to the coupled effects from other motions especially surge on pitch, leading to stretching of the slack mooring line. Thus, resulted into a higher line tension and motions. The values of pitch have also exceeded the critical limit for the design when impacted by a freak wave (DNV 2013). Whereas, in the taut mooring, the pitch is considerably low. Hence, taut mooring performs better than slack in freak wave case. Since the intensity of Draupner wave is too high, this results into higher platform responses in comparison to the regular waves considered in the present study. Thus, substantiating the need to consider these types of extreme waves in the design of FOWT.

3.4.1 Frequency domain analysis

A frequency domain investigation is also performed on the time history of the responses under the Draupner wave. As this wave contains different range of frequencies and wave heights, compared to the monochromatic regular waves considered, a Fast Fourier Transform (FFT) is

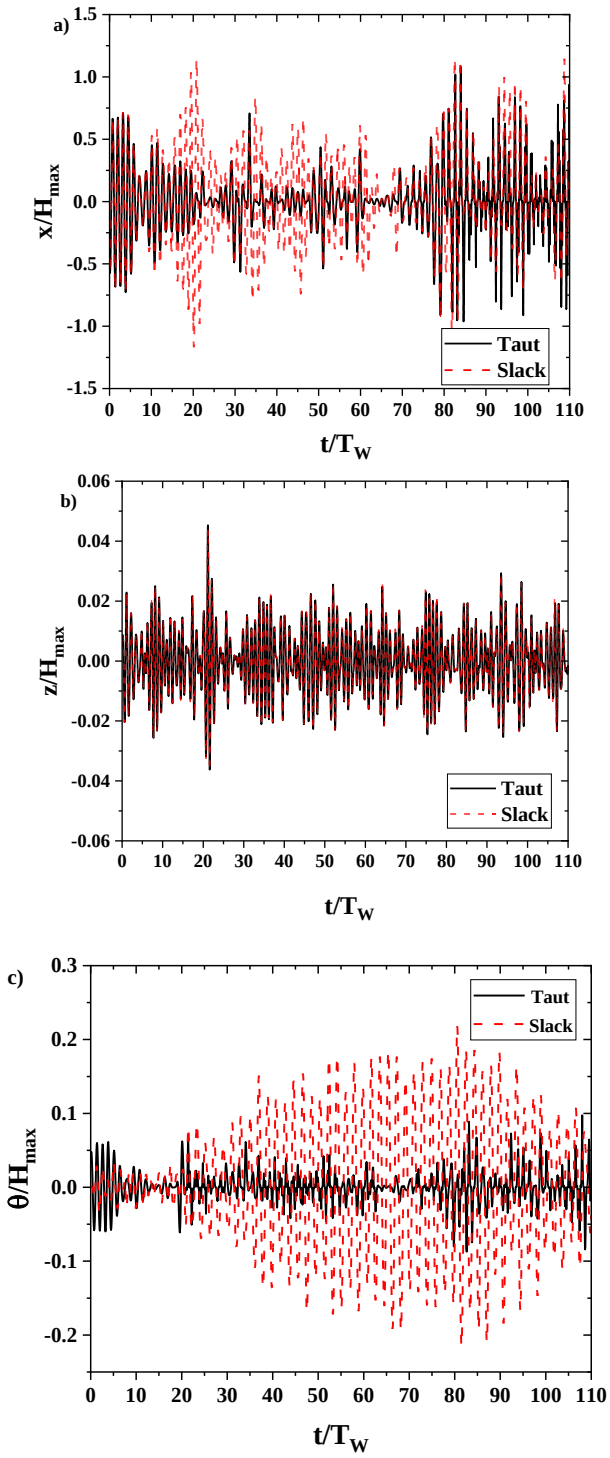

Fig. 13 Normalized response time series under freak wave impact: (a) Surge, (b) Heave and (c) Pitch (where, x is the surge, z is the heave, θ is the pitch)

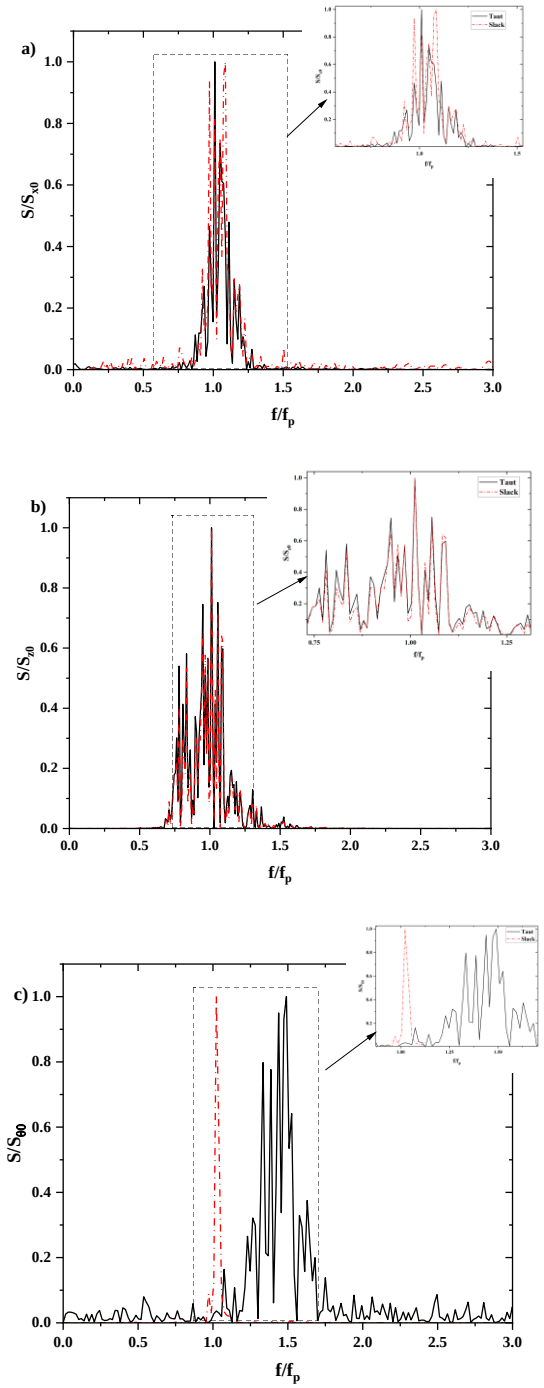

Fig. 14 Response energy spectrum for taut and slack mooring system under freak wave (a) Surge, (b) Heave, (c) Pitch (where S_x is the spectral density in surge, S_z is the spectral density in heave, S_θ is the spectral density in pitch, S_{i0} is the maximum spectral density amplitude in respective directions, f is the frequency, f_p is the peak frequencies in respective directions)

conducted to determine the peak frequencies that affect the responses. The response energy spectrums demonstrate the variation of response energy with varying frequencies (Fig. 14). On comparing the surge spectral density for the two mooring arrangements, slack mooring contributes to higher energy distribution. Though there is a difference in surge energy distribution (~3.2 times) between the two mooring arrangements, the maximum amplitude of the energy for taut mooring occurred at the freak wave frequency ($f/f_p = 1$). In contrast, the heave energy distribution is slightly away from the freak wave energy distribution (Fig. 14(b)). The time series plots also show a similar trend. The possible reason could be due to the interaction of freak wave trough on the heave response, which caused the phase shift of the peak frequency. The percentage difference in the heave energy distribution for the two mooring arrangements is insignificant (1%) compared to other responses. The pitch spectral densities plotted in the Fig. 14(c) demonstrate that the maximum pitch amplitude is having a deviation for the slack mooring configuration. These deviations are also observed in Li *et al*. (2020).

3.5 Effect of freak wave on Froude-Krylov force

The impact of Draupner wave on SPAR-type FOWT in terms of force is also investigated in the present study. It is noted that the force also shows a similar behaviour as that of the motions. From Fig. 15, the magnitude of this force is observed to be slightly more for the slack mooring arrangement. This can be due to the presence of un-stretched mooring line length and variation in stiffness. The magnitude for force in surge and pitch are comparatively higher as freak wave influence is more in these directions (Figs. 15(a) and 15(c)). Even though there is a marginal difference in force in both the configurations, the force got peaked at the same time instant (near the Draupner wave crest – $t/T_w \sim 21$). Compared to the regular wave, Draupner wave caused a significant increment in the wave loads (nearly 10 times). The study hence shows the importance of consideration of the freak wave scenarios in the design of FOWT.

Usually, the freak waves are numerically generated using spectrums under modulation methods where the effects of non-linearity are not taken into consideration for easiness (without considering the wave's instantaneous position change and the wet surface of the platform). These are discussed in Li *et al.* (2023). The freak wave scenario is highly non-linear and the variation in the instantaneous platform motions will be too rapid. This can arise higher order terms and non-linearity in FK forces along with Morison drag and 2nd order diffraction forces (Kim *et al*. 2018, 2021). The present study is based on linear potential flow theory, these non-linearities may not be captured completely and therefore, the results obtained should be applied with caution for freak wave conditions.

4. Conclusions

In the present study, the hydrodynamic investigations are carried out to determine the motion response and forces of a SPAR-type FOWT with taut and slack mooring configurations. The importance of this study lies in two aspects. Firstly, the comprehensive parametric investigations for a set of regular wave parameters provide insights on the behaviour of the SPAR FOWT. Secondly, the interaction of freak wave on the responses of FOWT is performed to check the robustness of the system. The major conclusions and observations from the current study are summarised here:

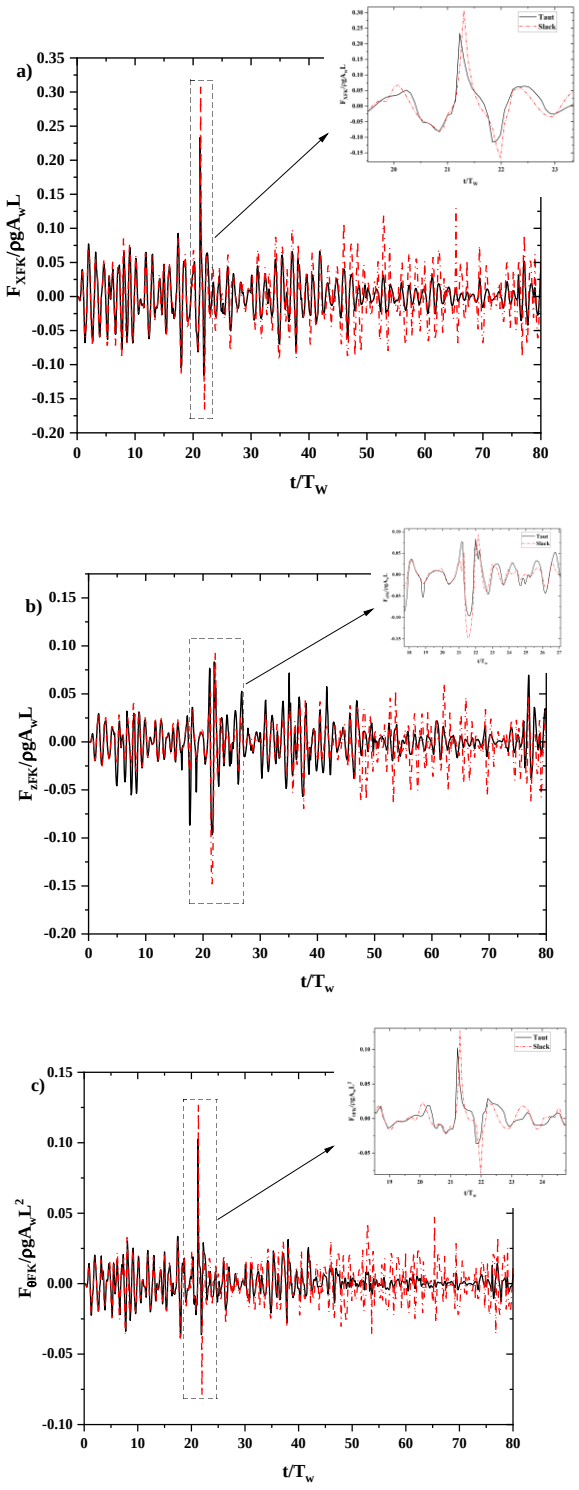

Fig. 15 Variation of Froude Krylov force/ moment for different mooring systems under freak wave in a) Surge, (b) Heave, (c) Pitch

- The maximum responses for a taut mooring configuration tend to increase with the increase in wave height and period for surge and heave, whereas pitch showed a decreasing trend under regular wave conditions.
- A 5% reduction in pitch motion is noticed for the slack mooring configuration in regular waves; however, the other two responses show feeble difference when compared to taut mooring configuration. There is an influence of lower period waves on surge in slack mooring arrangement.
- The motions are influenced by different mooring arrangements under different wave parameters, but this variation is not pronounced notably when the natural frequencies of the system coincide with the wave frequency even under different mooring arrangements.
- Froude-Krylov force tends to be non-linear due to the tapered portion of the FOWT. But it has insignificant difference among the taut and slack mooring line configurations. When the wave period is close to the natural period of FOWT, there is a sudden increase in this force for taut mooring configuration due to the consequence of different motion response.
- The freak wave has a significant effect on the surge of the slack configuration, as it drifts the platform to a larger offset due to more un-stretched length. The heave response for both the configurations shows an out-of-phase with the freak wave. The pitch is noticed to exceed its critical value during freak wave interaction. It has also increased the wave loads on the platform significantly.
- The study shows that the translational motions are better arrested by a slack mooring arrangement during normal sea states but under freak wave scenarios, taut mooring arrangement provides an effective station-keeping by offering more restrains in all DOFs.
- The study demonstrates the importance of considering the freak wave scenarios in the design and thereby improving the robustness of the FOWT system.

The study portrays the importance of considering several factors that affect the responses of the SPAR FOWT. As the current study uses a linear potential flow solver, the non-linear motions and forces due to the instantaneous wetted surface of the platform that influence the design of a floating offshore platform are not taken into consideration. However, there is still a need to examine by taking into account the non-linear behaviour beyond the still water level especially for the freak wave case. The mooring line tension assessment is also critical for understanding the overall engineering designs and operational strategies. Further investigations in this direction are suggested to be performed for enhancing the safety and reliability of FOWT system.

Acknowledgments

Authors would like to thank and acknowledge the funding received from NIOT, MoES, Government of India through Project No. NIOT/F&A/DOM-V5-01. Also, we are grateful to Prof. Sverre Haver (University of Stavanger) for sharing the Draupner wave time series.

References

Agarwal, A.K. and Jain, A.K. (2003), "Dynamic behavior of offshore spar platforms under regular sea waves", *Ocean Eng.*, **30**(4), 487-516. https://doi.org/10.1016/S0029-8018(02)00034-3.

ANSYS, A.Q.W.A. (2018), Aqwa Theory Manual. ANSYS, Inc., Canonsburg, PA, USA.

Aggarwal, N., Manikandan, R. and Saha, N. (2017), "Nonlinear short term extreme response of spar type floating offshore wind turbines", *Ocean Eng*., **130**, 199-209. https://doi.org/10.1016/j.oceaneng.2016.11.062.

Arya, T., Srineash, V.K. and Behera, M.R. (2023a), "Modeling of SPAR platform using soft mooring system", *Proceedings of the ICSOS International Conference on Ships and Offshore Structures*, Yantai, China, September (*presented*).

Atcheson, M., Garrad, A., Cradden, L., Henderson, A., Matha, D., Nichols, J., Roddier, D. and Sandberg, J. (2016), *Floating Offshore Wind Energy*, Springer International Publishing, New York, USA. https://doi.org/10.1007/978-3-319-29398-1.

Azcona, J. and Vittori, F. (2019), "Mooring system design for the 10 MW triple spar floating wind turbine at a 180 m sea depth location", *J. Physics: Conference Series*, **1356**(1), 012003. https://doi.org/10.1088/1742-6596/1356/1/012003.

Bach-Gansmo, M.T., Garvik, S.K., Thomsen, J.B. and Andersen, M.T. (2020), "Parametric study of a taut compliant mooring system for a FOWT compared to a catenary mooring", *J. Mar. Sci. Eng.*, **8**(6), 431. https://doi.org/10.3390/jmse8060431.

Barrera, C., Guanche, R. and Losada, I.J. (2019), "Experimental modelling of mooring systems for floating marine energy concepts", *Mar. Struct*., **63**,153-180. https://doi.org/10.1016/j.marstruc.2018.08.003.

Borlet, R. M. (2016), "Design and optimization of mooring systems for floating wind turbines", Master's thesis, NTNU, Norway.

Brito, M., Ferreira, R.M.L., Teixeira, L. Neves, M.G. and Canelas, R.B. (2020), "Experimental investigation on the power capture of an oscillating wave surge converter in unidirectional waves", *Renew. Energ*., **151**, 975-992. https://doi.org/10.1016/j.renene.2019.11.094.

Bruun, P. (1994), "Freak waves in the ocean and along shores, including impacts on fixed and floating structures", *J. Coast. Res.*, 163-175. https://www.jstor.org/stable/25735596.

Chakrabarti, S.K. (1987), *Hydrodynamics of offshore structures*, WIT press, Ashurst, UK.

Collu, M. and Borg, M. (2016), *Design of floating offshore wind turbines*, In Offshore wind farms, 359-385. https://doi.org/10.1016/B978-0-08-100779-2.00011-8.

Det, N. (2013), "DNV offshore standard DNV-OS-J101, design of offshore wind turbine", *Technical Standard*, 134-135, Norway.

Edwards, E.C., Holcombe, A., Brown, S., Ransley, E., Hann, M. and Greaves, D. (2023), "Evolution of floating offshore wind platforms: A review of at-sea devices", *Renew. Sust. Energ. Rev.*, **183**, 113416. https://doi.org/10.1016/j.rser.2023.113416.

Esteban, M.D., Diez, J.J., López, J.S. and Negro, V. (2011), "Why offshore wind energy?", *Renew. Energ.*, **36**(2), 444-450. https://doi.org/10.1016/j.renene.2010.07.009.

Ghafari, H.R., Ketabdari, M.J., Ghassemi, H. and Homayoun, E. (2019), "Numerical study on the hydrodynamic interaction between two floating platforms in Caspian Sea environmental conditions", *Ocean Eng.*, **188**, 106273. https://doi.org/10.1016/j.oceaneng.2019.106273.

Ghigo, A., Niosi, F., Paduano, B., Bracco, G. and Mattiazzo, G. (2022), "Mooring system design and analysis for a floating offshore wind turbine in Pantelleria", In *Turbo Expo: Power for Land, Sea, and Air*, **86137**, V011T38A021. American Society of Mechanical Engineers, June. https://doi.org/10.1115/GT2022-83219.

Hayer, S. and Andersen, O.J. (2000), "Freak waves: Rare realizations of a typical population or typical realizations of a rare population?", *Proceedings of the ISOPE International Ocean and Polar Engineering Conference (pp. ISOPE-I)*, Seattle, Washington, USA, May.

Hegde, P. and Nallayarasu, S. (2023), "Hydrodynamic response of buoy form spar with heave plate near the free surface validated with experiments", *Ocean Eng*., **269**, 113580. https://doi.org/10.1016/j.oceaneng.2022.113580.

Jang, H. and Kim, M. (2020), "Effects of nonlinear FK (Froude-Krylov) and hydrostatic restoring forces on arctic-spar motions in waves", *Int. J. Naval Architect. Ocean Eng.*, **12**, 297-313. https://doi.org/10.1016/j.ijnaoe.2020.01.002.

Jonkman, J. (2010), *Definition of the Floating System for Phase IV of OC3, (No. NREL/TP-500-47535). National Renewable Energy Lab. (NREL)*, Golden, CO (United States), May.

Kim, H.J., Lee, K.S. and Jang, B.S. (2018), "A linearization coefficient for Morison force considering the intermittent effect due to free surface fluctuation", *Ocean Eng.*, **159**, 139-149. https://doi.org/10.1016/j.oceaneng.2018.04.025.

Kim, S.J., Koo, W. and Kim, M.H. (2021), "The effects of geometrical buoy shape with nonlinear Froude-Krylov force on a heaving buoy point absorber", *Int. J. Naval Architect. Ocean Eng.*, **13**, 86-101. https://doi.org/10.1016/j.ijnaoe.2021.01.008.

Kota, R.S., Greiner, W. and D'Souza, R.B. (1999), "Comparative assessment of steel and polyester moorings in ultradeep water for spar-and semi-based production platforms", *Proceedings of the Offshore Technology Conference*, OTC, May. https://doi.org/10.4043/10909-MS.

Le Méhauté, B. (1976), *An introduction to hydrodynamics and water waves*, Springer Science & Business Media, Germany.

Li, Y., Qu, X., Liu, L., Xie, P., Yin, T. and Tang, Y. (2020), "A numerical prediction on the transient response of a spar-type floating offshore wind turbine in freak waves", *J. Offshore Mech. Arct.*, **142**(6), 062004. https://doi.org/10.1115/1.4047202.

Li, Y., Li, H., Wang, Z., Li, Y., Wang, B. and Tang, Y. (2023), "The dynamic response of a Spar-type floating wind turbine under freak waves with different properties", *Mar. Struct.*, **91**, 103471. https://doi.org/10.1016/j.marstruc.2023.103471.

Li, H., Li, Y., Li, G., Zhu, Q., Wang, B. and Tang, Y. (2024), "Transient tower and blade deformations of a Spar-type floating wind turbine in freak waves", *Ocean Eng.*, **294**, 116801. https://doi.org/10.1016/j.oceaneng.2024.116801.

Luo, M., Koh, C.G., Lee, W.X., Lin, P. and Reeve, D.E. (2020), "Experimental study of freak wave impacts on a tension-leg platform", *Mar. Struct.*, **74**, 102821. https://doi.org/10.1016/j.marstruc.2020.102821.

Morton, A., Greenfield, P., Harvey, F., Lakhani, N. and Carrington, D. (2023), "Cop28 landmark deal agreed to 'transition away'from fossil fuels", The Guardian, https://www. theguardian. com/environment/2023/dec/13/cop28-landmark-deal-agreed-to-transition-away-from-fossil-fuels.

Nallayarasu, S. and Saravanapriya, S. (2013), "Experimental and numerical investigation on hydrodynamic response of spar with wind turbine under regular waves", *Int. J. Ocean Climate Syst.*, **4**(4), 239-260. https://doi.org/10.1260/1759-3131.4.4.239.

Nallayarasu, S. and Kumar, N.S. (2017), "Experimental and numerical investigation on hydrodynamic response of buoy form spar under regular waves", *Ships Offshore Struct.*, **12**(1), 19-31. https://doi.org/10.1080/17445302.2015.1099227.

Proskovics, R. (2015), "Dynamic response of spar-type offshore floating wind turbines", Ph.D. Dissertation, University of Strathclyde, UK.

Qu, X., Li, Y., Tang, Y., Hu, Z., Zhang, P. and Yin, T. (2020), "Dynamic response of spar-type floating offshore wind turbine in freak wave considering the wave-current interaction effect", *Appl. Ocean Res.*, **100**, 102178. https://doi.org/10.1016/j.apor.2020.102178.

Ramachandran, G.K.V., Robertson, A., Jonkman, J.M. and Masciola, M.D. (2013), "Investigation of response amplitude operators for floating offshore wind turbines", *Proceedings of the ISOPE International Ocean and Polar Engineering Conference* (pp. ISOPE-I). ISOPE, Alaska, June.

Ravichandran, N. and Bidorn, B. (2024), "Study on the dynamic response of offshore triceratops under freak waves", *J. Mar. Sci. Eng*., **12**(8), 1260. https://doi.org/10.3390/jmse12081260.

Rajeswari, K. and Nallayarasu, S. (2022), "Experimental and numerical investigation on the suitability of semi-submersible floaters to support vertical axis wind turbine", *Ship. Offshore Struct*., **17**(8), 1743-1754. https://doi.org/10.1080/17445302.2021.1938800.

Riggs, H.R., Ertekin, R.C. and Mills, T.R.J. (1999), "Impact of stiffness on the response of a multimodule mobile offshore base", *Int. J. Offshore Polar Eng*., **9**(2).

Rony, J.S., Chaitanya Sai, K. and Karmakar, D. (2023), "Numerical investigation of offshore wind turbine combined with wave energy converter", *Mar. Syst. Ocean Technol.*, **18**(1), 14-44. https://doi.org/10.1007/s40868-023-00127-4.

Ruzzo, C., Muggiasca, S., Malara, G., Taruffi, F., Belloli, M., Collu, M., Li, L., Brizzi, G. and Arena, F. (2021), "Scaling strategies for multi-purpose floating structures physical modeling: state of art and new

perspectives", *Appl. Ocean Res.*, **108**, 102487. https://doi.org/10.1016/j.apor.2020.102487.
Sand, S.E., Hansen, N.O., Klinting, P., Gudmestad, O.T. and Sterndorff, M.J. (1990), "Freak wave kinematics", *Water wave kinematics*, 535-549. https://doi.org/10.1007/978-94-009-0531-3_34.
Song, C.Y., Moon, C.I. and Cha, J.H. (2012), "Mooring effects on dynamic behavior of sub-structure for floating-type offshore wind turbine system", *Proceedings of the ISOPE International Ocean and Polar Engineering Conference*, ISOPE, Rhodes, Greec, June.
Tang, Y.G., Zhang, S.X., Zhang, R.Y. and Liu, H.X. (2007), "Development of study on the dynamic characteristics of deep water mooring system", *J. Mar. Sci. Appl.*, **6**(3), 17-23. https://doi.org/10.1007/s11804-007-7016-2.
Thomas, A., VK, S. and Behera, M.R. (2023b), "Numerical investigation of a SPAR type floating offshore wind turbine platform under extreme waves", *Proceedings of the International Conference on Offshore Mechanics and Arctic Engineering*, **87578**, V001T01A013. American Society of Mechanical Engineers, Exeter, UK, December. https://doi.org/10.1115/IOWTC2023-119363.
Xiang, G., Xiang, X. and Yu, X. (2022), "Dynamic response of a spar-type floating wind turbine foundation with taut mooring system", *J. Mar. Sci. Eng.*, **10**(12), 1907. https://doi.org/10.3390/jmse10121907.
Xue, S., Xu, G., Xie, W., Xu, L. and Jiang, Z. (2023), "Characteristics of freak wave and its interaction with marine structures: A review", *Ocean Eng*., **287**, 115764. https://doi.org/10.1016/j.oceaneng.2023.115764.
Xu, X. and Day, S. (2021), "Experimental investigation on dynamic responses of a spar-type offshore floating wind turbine and its mooring system behaviour", *Ocean Eng.*, **236**, 109488. https://doi.org/10.1016/j.oceaneng.2021.109488.
Yang, R.Y., Wang, C.W., Huang, C.C., Chung, C.H., Chen, C.P. and Huang, C.J. (2022), "The 1: 20 scaled hydraulic model test and field experiment of barge-type floating offshore wind turbine system", *Ocean Eng.*, **247**, 110486. https://doi.org/10.1016/j.oceaneng.2021.110486.
Zeng, F., Zhang, N., Huang, G., Gu, Q. and He, M. (2023), "Experimental study on dynamic response of a floating offshore wind turbine under various freak wave profiles", *Mar. Struct.*, **88**, 103362. https://doi.org/10.1016/j.marstruc.2022.103362.

MK